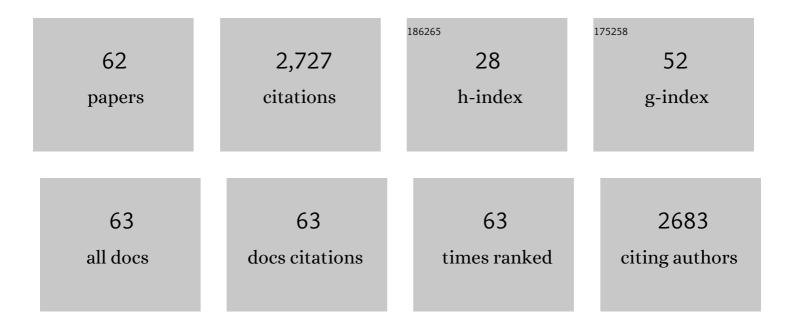
## Joan Vila-Comamala

List of Publications by Year in descending order

Source: https://exaly.com/author-pdf/3134372/publications.pdf Version: 2024-02-01



#	Article	IF	CITATIONS
1	An achromatic X-ray lens. Nature Communications, 2022, 13, 1305.	12.8	19
2	Fabrication of X-ray Gratings for Interferometric Imaging by Conformal Seedless Gold Electroplating. Micromachines, 2021, 12, 517.	2.9	14
3	Laboratory X-ray interferometry imaging with a fan-shaped source grating. Optics Letters, 2021, 46, 3693.	3.3	9
4	High sensitivity X-ray phase contrast imaging by laboratory grating-based interferometry at high Talbot order geometry. Optics Express, 2021, 29, 2049.	3.4	35
5	Generation of highly mutually coherent hard-x-ray pulse pairs with an amplitude-splitting delay line. Physical Review Research, 2021, 3, .	3.6	7
6	Highâ€Aspectâ€Ratio Grating Microfabrication by Platinumâ€Assisted Chemical Etching and Gold Electroplating. Advanced Engineering Materials, 2020, 22, 2000258.	3.5	32
7	Metal assisted chemical etching of silicon in the gas phase: a nanofabrication platform for X-ray optics. Nanoscale Horizons, 2020, 5, 869-879.	8.0	50
8	Pushing the Limits of Bottom-Up Gold Filling for X-ray Grating Interferometry. Journal of the Electrochemical Society, 2020, 167, 132504.	2.9	20
9	X-ray phase tomography with near-field speckles for three-dimensional virtual histology. Optica, 2020, 7, 1221.	9.3	37
10	Light Yield Enhancement of 157-Gadolinium Oxysulfide Scintillator Screens for the High-Resolution Neutron Imaging. MethodsX, 2019, 6, 107-114.	1.6	18
11	Towards sub-micrometer high aspect ratio X-ray gratings by atomic layer deposition of iridium. Microelectronic Engineering, 2018, 192, 19-24.	2.4	39
12	Tunable X-ray speckle-based phase-contrast and dark-field imaging using the unified modulated pattern analysis approach. Journal of Instrumentation, 2018, 13, C05005-C05005.	1.2	8
13	Advanced X-ray phase-contrast and dark-field imaging with the unified modulated pattern analysis (UMPA). Microscopy and Microanalysis, 2018, 24, 22-23.	0.4	1
14	Development of Laboratory Grating-based X-ray Phase Contrast Microtomography for Improved Pathology. Microscopy and Microanalysis, 2018, 24, 192-193.	0.4	6
15	High aspect ratio metal microcasting by hot embossing for X-ray optics fabrication. Microelectronic Engineering, 2017, 176, 6-10.	2.4	27
16	Systematic efficiency study of line-doubled zone plates. Microelectronic Engineering, 2017, 177, 25-29.	2.4	25
17	Effect of isopropanol on gold assisted chemical etching of silicon microstructures. Microelectronic Engineering, 2017, 177, 59-65.	2.4	35
18	High-aspect ratio silicon structures by displacement Talbot lithography and Bosch etching. Proceedings of SPIE, 2017, , .	0.8	18

JOAN VILA-COMAMALA

#	Article	IF	CITATIONS
19	Hot embossing of Au- and Pb-based alloys for x-ray grating fabrication. Journal of Vacuum Science and Technology B:Nanotechnology and Microelectronics, 2017, 35, .	1.2	14
20	Dynamic Pore-scale Reservoir-condition Imaging of Reaction in Carbonates Using Synchrotron Fast Tomography. Journal of Visualized Experiments, 2017, , .	0.3	3
21	X-ray phase microtomography with a single grating for high-throughput investigations of biological tissue. Biomedical Optics Express, 2017, 8, 1257.	2.9	19
22	High resolution beam profiling of X-ray free electron laser radiation by polymer imprint development. Optics Express, 2017, 25, 30686.	3.4	23
23	Transmission x-ray microscopy at Diamond-Manchester I13 Imaging Branchline. AIP Conference Proceedings, 2016, , .	0.4	3
24	Phase retrieval by coherent modulation imaging. Nature Communications, 2016, 7, 13367.	12.8	125
25	<i>In Situ</i> Heater Design for Nanoscale Synchrotron-Based Full-Field Transmission X-Ray Microscopy. Microscopy and Microanalysis, 2015, 21, 290-297.	0.4	5
26	The Effect of Nitrate on Salt Layers in Pitting Corrosion of 304L Stainless Steel. Journal of the Electrochemical Society, 2015, 162, C457-C464.	2.9	24
27	Three-dimensional characterization of electrodeposited lithium microstructures using synchrotron X-ray phase contrast imaging. Chemical Communications, 2015, 51, 266-268.	4.1	133
28	Full-field X-ray reflection microscopy of epitaxial thin-films. Journal of Synchrotron Radiation, 2014, 21, 1252-1261.	2.4	41
29	Fresnel zone plate stacking in the intermediate field for high efficiency focusing in the hard X-ray regime. Optics Express, 2014, 22, 28142.	3.4	35
30	Characterization of x-ray phase vortices by ptychographic coherent diffractive imaging. Optics Letters, 2014, 39, 5281.	3.3	40
31	Coherent X-Ray Imaging of Collagen Fibril Distributions within Intact Tendons. Biophysical Journal, 2014, 106, 459-466.	0.5	12
32	Three-Dimensional Microstructural Imaging of Sulfur Poisoning-Induced Degradation in a Ni-YSZ Anode of Solid Oxide Fuel Cells. Scientific Reports, 2014, 4, 5246.	3.3	33
33	X-ray computed tomography of the anterior cruciate ligament and patellar tendon. Muscles, Ligaments and Tendons Journal, 2014, 4, 238-44.	0.3	17
34	Ion beam lithography for Fresnel zone plates in X-ray microscopy. Optics Express, 2013, 21, 11747.	3.4	35
35	Angular spectrum simulation of X-ray focusing by Fresnel zone plates. Journal of Synchrotron Radiation, 2013, 20, 397-404.	2.4	38
36	Translation position determination in ptychographic coherent diffraction imaging. Optics Express, 2013, 21, 13592.	3.4	242

JOAN VILA-COMAMALA

#	Article	IF	CITATIONS
37	<i>In-situ</i> observation of nickel oxidation using synchrotron based full-field transmission X-ray microscopy. Applied Physics Letters, 2013, 102, .	3.3	14
38	Examining Effects of Sulfur Poisoning on Ni/YSZ Solid Oxide Fuel Cell Anodes Using Synchrotron-Based X-Ray Imaging Techniques. , 2013, , .		0
39	Role of the illumination spatial-frequency spectrum for ptychography. Physical Review B, 2012, 86, .	3.2	93
40	Zone-doubled Fresnel zone plates for high-resolution hard X-ray full-field transmission microscopy. Journal of Synchrotron Radiation, 2012, 19, 705-709.	2.4	59
41	Ultra-high resolution zone-doubled †diffractive X-ray optics for the multi-keV regime. Optics Express, 2011, 19, 175.	3.4	114
42	Characterization of high-resolution diffractive X-ray optics by ptychographic coherent diffractive imaging. Optics Express, 2011, 19, 21333.	3.4	166
43	Coherent x-ray diffraction imaging of paint pigment particles by scanning a phase plate modulator. New Journal of Physics, 2011, 13, 103022.	2.9	4
44	High-efficiency Fresnel zone plates for hard X-rays by 100â€keV e-beam lithography and electroplating. Journal of Synchrotron Radiation, 2011, 18, 442-446.	2.4	83
45	High aspect ratio nanostructuring by high energy electrons and electroplating. Microelectronic Engineering, 2011, 88, 2259-2262.	2.4	25
46	Characterization of a 20-nm hard x-ray focus by ptychographic coherent diffractive imaging. Proceedings of SPIE, 2011, , .	0.8	0
47	3D Nanostructuring of hydrogen silsesquioxane resist by 100 keV electron beam lithography. Journal of Vacuum Science and Technology B:Nanotechnology and Microelectronics, 2011, 29, 06F301.	1.2	19
48	Direct e-beam writing of high aspect ratio nanostructures in PMMA: A tool for diffractive X-ray optics fabrication. Microelectronic Engineering, 2010, 87, 1052-1056.	2.4	28
49	Ptychographic characterization of the wavefield in the focus of reflective hard X-ray optics. Ultramicroscopy, 2010, 110, 325-329.	1.9	117
50	Scanning transmission X-ray microscopy with a fast framing pixel detector. Ultramicroscopy, 2010, 110, 1143-1147.	1.9	33
51	Beam-induced damage on diffractive hard X-ray optics. Journal of Synchrotron Radiation, 2010, 17, 786-790.	2.4	8
52	High Spatial Resolution STXM at 6.2 keV Photon Energy. , 2010, , .		4
53	Direct e-beam writing of dense and high aspect ratio nanostructures in thick layers of PMMA for electroplating. Nanotechnology, 2010, 21, 295303.	2.6	92
54	Dense high aspect ratio hydrogen silsesquioxane nanostructures by 100 keV electron beam lithography. Nanotechnology, 2010, 21, 285305.	2.6	42

JOAN VILA-COMAMALA

#	Article	IF	CITATIONS
55	Reconstruction of an astigmatic hard X-ray beam and alignment of K-B mirrors from ptychographic coherent diffraction data. Optics Express, 2010, 18, 23420.	3.4	120
56	Phase-contrast tomography at the nanoscale using hard x rays. Physical Review B, 2010, 81, .	3.2	115
57	Advanced thin film technology for ultrahigh resolution X-ray microscopy. Ultramicroscopy, 2009, 109, 1360-1364.	1.9	111
58	Spatially resolved strain within a single SiGe island investigated by Xâ€ray scanning microdiffraction. Physica Status Solidi (A) Applications and Materials Science, 2009, 206, 1829-1832.	1.8	12
59	Beam-shaping condenser lenses for full-field transmission X-ray microscopy. Journal of Synchrotron Radiation, 2008, 15, 106-108.	2.4	50
60	Silicon Fresnel zone plates for high heat load X-ray microscopy. Microelectronic Engineering, 2008, 85, 1241-1244.	2.4	14
61	Zone-Doubling Technique to Produce Ultrahigh-Resolution X-Ray Optics. Physical Review Letters, 2007, 99, 264801.	7.8	154
62	Nanofabrication of Fresnel zone plate lenses for X-ray optics. Microelectronic Engineering, 2006, 83, 1355-1359.	2.4	7